Giant Enhancement of Unconventional Photon Blockade in a Dimer Chain

You Wang,[1,*] W. Verstraelen,[1,*] Baile Zhang,[1,2,†] Timothy C. H. Liew,[1,3,‡] and Y. D. Chong[1,2,§]
[1]Division of Physics and Applied Physics, School of Physical and Mathematical Sciences, Nanyang Technological University, Singapore 637371, Singapore
[2]Centre for Disruptive Photonic Technologies, School of Physical and Mathematical Sciences, Nanyang Technological University, Singapore 637371, Singapore
[3]MajuLab, International Joint Research Unit UMI 3654, CNRS, Université Côte d'Azur, Sorbonne Université, National University of Singapore, Nanyang Technological University, Singapore 637371, Singapore

(Received 7 July 2021; accepted 15 November 2021; published 10 December 2021)

Unconventional photon blockade refers to the suppression of multiphoton states in weakly nonlinear optical resonators via the destructive interference of different excitation pathways. It has been studied in a pair of coupled nonlinear resonators and other few-mode systems. Here, we show that unconventional photon blockade can be greatly enhanced in a chain of coupled resonators. The strength of the nonlinearity in each resonator needed to achieve unconventional photon blockade is suppressed exponentially with lattice size. The analytic derivation, based on a weak drive approximation, is validated by wave function Monte Carlo simulations. These findings show that customized lattices of coupled resonators can be powerful tools for controlling multiphoton quantum states.

DOI: 10.1103/PhysRevLett.127.240402

Photon blockade—the use of optical nonlinearity to suppress multiphoton quantum states—is a mechanism for generating nonclassical light through coherent optical illumination [1–4], with applications in quantum computing, quantum simulation, and other emerging quantum technologies [5–10]. The conventional photon blockade effect requires strong optical nonlinearities, as it relies on interactions between resonant single-photon states and off-resonant multiphoton states, so the interaction strength has to be much larger than the cavity decay rate. This regime can be achieved in cavity QED systems [6,11–21], superconducting circuits [22,23], optomechanical resonators [23–26], and other systems [27,28]. Weak nonlinearities, however, are much easier to realize, such as in resonators made of common nonlinear optical materials. Remarkably, it is possible to efficiently suppress multiphoton states even in the weakly nonlinear regime, through the phenomenon of unconventional photon blockade (UPB). Liew and Savona showed some years ago that in a system of two coupled nonlinear resonators, careful parameter tuning can enable destructive interference between different excitation pathways for the formation of two-photon states in one resonator, even when the photon interaction strength is smaller than the cavity decay rate [29]. Subsequently, the conditions for UPB to occur have been extensively studied [30–35], and the phenomenon has been realized in experiments [36,37]. Other ways of realizing UPB using different setups and different quantum interference schemes have also been proposed [31,38–48], and similar ideas have been explored for other forms of multiphoton state control in weakly nonlinear systems, such as for creating entangled photon sources [49,50].

In the context of classical optics and photonics, synthetic lattices such as photonic crystals [51] and photonic metamaterials [52,53] have proven to be versatile platforms for wave manipulation. By offering a richer set of customizable degrees of freedom, such as lattice symmetries, they have the potential to outperform devices composed of individual or a few coupled optical cavities, or even access qualitatively different behaviors. For instance, photonic lattices can host "bound states in the continuum," whose decay rates vanish due to destructive interference of numerous decay pathways [54].

In this Letter, we show that a lattice of coupled resonators can achieve UPB at much lower levels of optical nonlinearity than previously studied two-resonator setups. We consider resonators arranged in a dimer chain, or Su-Schrieffer-Heeger (SSH) lattice, a one-dimensional model whose single-particle properties have been extensively studied [55]. By analyzing multiphoton states in this system and exploiting lattice features such as chiral symmetry, we derive analytic expressions for the one- and two-photon quantum amplitudes to leading order in the intercell coupling. Remarkably, we find that the nonlinear Kerr coefficient required for UPB in a given signal resonator is suppressed exponentially in the number of sites. Our theory predicts the required resonator frequency detunings and cavity decay rates, which form a striking pattern of complex roots in a 2D parameter space. For the limiting case of a dimer (i.e., two resonators), our formulas reproduce previous results [31]. Wave function Monte Carlo (WFMC) simulations of the

multiphoton system agree well with the analytic results, and help quantify the limits on photon antibunching imposed by pure dephasing. Recently, two-mode UPB has been demonstrated with quantum dot cavities [36] and superconducting circuits [37], and our findings may help in designing lattice-based single-photon sources on weakly-nonlinear platforms such as silicon photonics [39,56].

Consider coupled optical resonators with identical physical properties and weak Kerr-type nonlinearity, arranged in a dimer chain (or SSH lattice [55]) as shown in Fig. 1(a). The number of sites N is even. In the absence of driving and dissipation, the Hamiltonian is $\mathcal{H}_0 = \mathcal{H}_c + \mathcal{H}_p + \mathcal{H}_{nl}$, where

$$\mathcal{H}_c = \left(\sum_{j=1}^{N/2} a_{2j-1}^\dagger a_{2j} + t\sum_{j=1}^{N/2-1} a_{2j}^\dagger a_{2j+1}\right) + \text{H.c.},$$
$$\mathcal{H}_p = E\sum_{j=1}^{N} a_j^\dagger a_j, \qquad \mathcal{H}_{nl} = \alpha\sum_{j=1}^{N} a_j^\dagger a_j^\dagger a_j a_j. \tag{1}$$

Here, $a_j^{(\dagger)}$ is the photon annihilation (creation) operator on site j, t is the intercell hopping, E is the on-site single-photon energy, $\alpha \in \mathbb{R}$ is the Kerr coefficient, and H.c. stands for the Hermitian conjugate. The intracell hopping is normalized to unity (in nanophotonic systems, this is determined by local features such as inter-resonator spacings), so parameters such as E, α, and t are expressed relative to this energy scale. We choose positive couplings, but negative couplings can be dealt with by redefining the operators for even j. Note that although the SSH model is well known for hosting topologically protected single-particle eigenstates at boundaries and domain walls, this behavior is not used in the present work; our chain has no domain walls, and (since N is even) no single-particle topological end states. More pertinent is the SSH model's chiral symmetry, which ensures that the single-photon spectrum is symmetric around zero, giving rise to a family of noninteracting two-photon zero modes formed by pairs of upper- and lower-band single-photon states. This is a generalization of the single-dimer ($N = 2$) model, where a similar chiral symmetry is used to set up UPB [29].

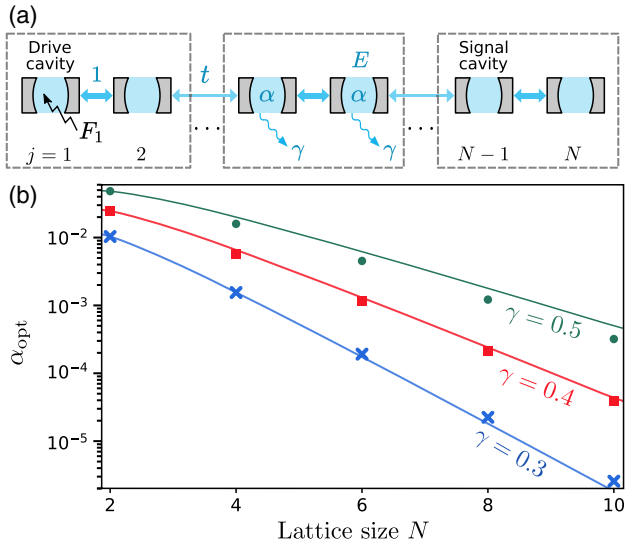

FIG. 1. (a) Schematic of a dimer chain of optical resonators. Site $j = 1$ is coherently driven, and site $N - 1$ is the signal resonator. Each resonator has single-photon energy E, Kerr coefficient α, and decay rate γ. Dashed boxes indicate the unit cells; intra- and intercell couplings are 1 and t, respectively. (b) Optimal Kerr coefficients for UPB in lattices of different N, with $t = 0.1$ and $\gamma = 0.3$, 0.4, 0.5. The solid curves show the analytic approximation (17), and the discrete data points are numerical solutions to the weak drive equations.

Let the sites be coherently driven by the Hamiltonian

$$\mathcal{H}_d = \sum_{j=1}^{N} F_j a_j^\dagger + \text{H.c.}, \tag{2}$$

where F_j is the excitation coefficient on site j. Figure 1(a) depicts the case where only the first site is driven, $F_j = F_1\delta_{1j}$. The evolution of the density matrix ρ is given by the Lindblad master equation [57]

$$i\hbar\frac{d\rho}{dt} = [\mathcal{H}_{\text{tot}}, \rho] + \frac{i\gamma}{2}\sum_{j=1}^{N}(2a_j\rho a_j^\dagger - a_j^\dagger a_j\rho - \rho a_j^\dagger a_j), \tag{3}$$

where $\mathcal{H}_{\text{tot}} = \mathcal{H}_0 + \mathcal{H}_d$. The terms in parentheses represent environmental interactions that induce (i) deterministic on-site decays and (ii) stochastic quantum jumps stemming from the fluctuation-dissipation theorem. Both of these effects will be accounted for when we later solve Eq. (3) using stochastic WFMC simulations [58–61]. For now, we pursue an approximate solution by neglecting the fluctuations and absorbing the deterministic decay terms into the Hamiltonian. We define

$$\mathcal{H}_p' = z\sum_{j=1}^{N} a_j^\dagger a_j, \quad \text{where } z = E - \frac{i\gamma}{2}, \tag{4}$$

and consider the semiclassical regime where time evolution is well described by the Schrödinger equation with the non-Hermitian Hamiltonian $\mathcal{H} = \mathcal{H}_c + \mathcal{H}_p' + \mathcal{H}_{nl}$. Flayac and Savona have argued that this is valid in the "weak drive" limit $F_j \to 0$, since stochastic jumps are rare when photon occupation numbers are low [40].

The steady state solution has the form

$$|\psi\rangle = \sum_{k=0}^{\infty} |\psi^{(k)}\rangle, \tag{5}$$

where $|\psi^{(k)}\rangle$ is the projection of the full wave function into the k-photon subspace ($|\psi^{(0)}\rangle$ is the vacuum state). In the

weak drive limit, the amplitude for the higher photon number states is negligible. Truncating at $k = 2$, we obtain [62]

$$|\psi^{(1)}\rangle = -\mathcal{H}^{-1}\mathcal{H}_+|\psi^{(0)}\rangle, \tag{6}$$

$$|\psi^{(2)}\rangle = -\mathcal{H}^{-1}\mathcal{H}_+|\psi^{(1)}\rangle, \tag{7}$$

where $\mathcal{H}_+ = \sum_j F_j a_j^\dagger$. For $k = 1$, we adopt the eigenstate basis of $\mathcal{H}_c^{(1)}$ (the projection of $\mathcal{H}_c$ to the 1-photon subspace), defined by

$$\mathcal{H}_c^{(1)}|\varphi_n\rangle = \epsilon_n|\varphi_n\rangle. \tag{8}$$

Hence, the solution to Eq. (6) can be written as

$$|\psi^{(1)}\rangle = \sum_n \frac{f_n|\varphi_n\rangle}{z+\epsilon_n}, \qquad f_n = \sum_{j=1}^{N} F_j\langle\varphi_n|j\rangle, \tag{9}$$

where $|j\rangle \equiv a_j^\dagger|\psi^{(0)}\rangle$ is the state in which only site j is occupied by a single photon. Details of the derivation are given in the Supplemental Material [62]. Next, for $k = 2$, we define a basis formed by tensor products of the single-particle eigenstates, $|\varphi_{mn}\rangle \equiv |\varphi_m\rangle \otimes |\varphi_n\rangle$, and seek perturbative solutions to Eq. (7) of the form

$$|\psi^{(2)}\rangle \approx |\psi_0^{(2)}\rangle + \alpha|\psi_1^{(2)}\rangle, \tag{10}$$

where the solution in the absence of nonlinearity is

$$|\psi_0^{(2)}\rangle = \frac{1}{\sqrt{2}}\sum_{mn}\frac{f_m f_n}{(z+\epsilon_m)(z+\epsilon_n)}|\varphi_{mn}\rangle, \tag{11}$$

and the perturbative correction can be shown to be [62]

$$|\psi_1^{(2)}\rangle = \sum_{imnpq}|\varphi_{mn}\rangle\frac{-\sqrt{2}f_p f_q\langle\varphi_{mn}|i,i\rangle\langle i,i|\varphi_{pq}\rangle}{(z+\epsilon_p)(z+\epsilon_q)(2z+\epsilon_m+\epsilon_n)}, \tag{12}$$

where $|i,i\rangle \equiv |i\rangle \otimes |i\rangle$.

Suppose only the first site is driven, so $f_n = F_1\langle\varphi_n|1\rangle$. The $N = 2$ lattice (i.e., a single dimer) is known to exhibit UPB in site 1, which serves as both the drive and signal resonator [29]. We will generalize this to larger N by demonstrating enhanced UPB on a designated signal resonator on site $N-1$ (i.e., one site away from the end of the chain, opposite to the drive cavity), as shown in Fig. 1(a). UPB shall be achieved if the equal time second-order photon correlation in the signal resonator,

$$g_s^{(2)}(0) = 2\frac{|\langle N-1,N-1|\psi^{(2)}\rangle|^2}{|\langle N-1|\psi^{(1)}\rangle|^4}, \tag{13}$$

vanishes. Note that plugging only Eq. (11) into Eq. (13) gives $g_s^{(2)}(0) = 1$ (i.e., in the linear regime the emission is always coherent).

If the intercell coupling is weak ($t \ll 1$), we can estimate the two-photon state by applying Laurent series expansions to Eqs. (11) and (12) in the domain $t < |z| < 1$. The derivation, given in the Supplemental Material [62], utilizes the chiral symmetry of $\mathcal{H}_c^{(1)}$. The result is

$$\begin{aligned}\langle N-1,N-1|\psi_0^{(2)}\rangle &\approx \frac{F_1^2}{\sqrt{2}}t^{N-2}z^2,\\ \langle N-1,N-1|\psi_1^{(2)}\rangle &\approx \frac{F_1^2}{\sqrt{2}}\frac{(-1)^{\frac{N}{2}+1}(N-3)!!t^{N-2}}{(N-2)!!(2z)^{N-1}}.\end{aligned} \tag{14}$$

Referring to Eq. (10), UPB is achieved when

$$\alpha \approx \frac{(-1)^{\frac{N}{2}}}{4}\frac{(N-2)!!}{(N-3)!!}(2z)^{N+1}. \tag{15}$$

Notably, this is independent of the drive amplitude F_1.

We now restrict our discussion to $\alpha > 0$ for simplicity of presentation (the $\alpha < 0$ case is very similar). From Eq. (15), $z/|z|$ is one of the $(N+1)$ complex roots of $(-1)^{N/2}$. We select the root with the most negative imaginary part, corresponding to the experimentally preferred situation where α/γ, the nonlinearity strength relative to the cavity decay rate, is minimal; choosing a different root would only slightly modify the following results. Then E and α can be expressed in terms of γ, as follows:

$$E = \frac{\gamma}{2}\cot\theta, \tag{16}$$

$$\alpha = \frac{1}{4}\frac{(N-2)!!}{(N-3)!!}(\gamma\csc\theta)^{N+1}, \tag{17}$$

$$\theta = \frac{N}{N+1}\frac{\pi}{2}. \tag{18}$$

For $N = 2$, this reproduces the previously derived single-dimer result [31]. For larger N, given any decay rate γ smaller than the intracell coupling strength (i.e., $\gamma < 1$), Eq. (17) states that the nonlinearity strength α required for UPB decreases exponentially with the lattice size N. This is the primary finding of the present work.

Instead of using the series expansions, we can solve the single-photon eigenproblem (8) numerically, and plug the results into the weak drive equations (9) and (11)–(12) to obtain the single-photon and two-photon wave functions. [This is more efficient than directly solving Eqs. (6)–(7) as it avoids a matrix inversion for each z.] Figure 1(b) plots the optimal Kerr coefficients versus lattice size N, as given by the analytic expression (solid curves) and the numerical

solutions to the weak drive equations (discrete points). We find good agreement between the two.

The vanishing of the two-photon signal for specific z is a robust feature, since these are exact zeros of the regular function $\langle N-1, N-1|\psi^{(2)}\rangle$ in the complex z plane. Although Eq. (17) gives approximate locations for the zeros, valid for $t \ll 1$, small corrections merely shift the zeros; they cannot be eliminated except by annihilation with poles arriving from elsewhere in the complex plane. To show this, Fig. 2 plots the complex argument of $\langle N-1, N-1|\psi^{(2)}\rangle$ versus z, obtained numerically from the weak drive equations for various N. Here and in the following numerical examples, we choose $t = 0.1$ and different α for each N. We observe phase singularities at discrete z points, corresponding to analytic zeros, occurring in the predicted pattern of roots of $(-1)^{N/2}$. With increasing N, smaller values of α are required for the zeros to appear at comparable $|z|$, as expected. Experimentally, the fact that the UPB effect originates from analytic zeros implies that it is robust against disorder, which merely shifts the optimal values of z [62].

To verify the above results, we perform WFMC simulations [58–61,63], which solve Eq. (3) including the effects of stochastic quantum jumps. Figure 3(a) compares the $g_s^{(2)}(0)$ calculated by the two methods, for a lattice of

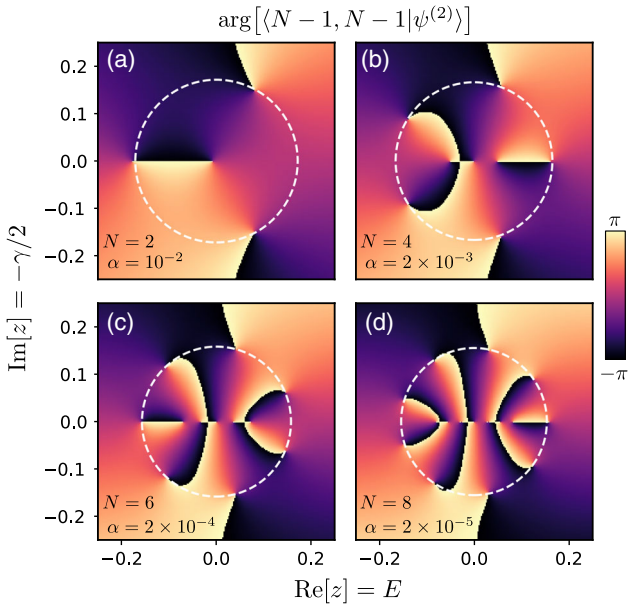

FIG. 2. Complex argument of $\langle N-1, N-1|\psi^{(2)}\rangle$, the two-photon amplitude in the signal resonator, plotted versus $\mathrm{Re}[z] = E$ and $\mathrm{Im}[z] = -\gamma/2$. The heat maps are obtained by solving the weak drive equations numerically, without the analytic approximations, using intracell coupling $t = 0.1$ and different values of N, α: (a) $N = 2$ with $\alpha = 10^{-2}$, (b) $N = 4$ with $\alpha = 2 \times 10^{-3}$, (c) $N = 6$ with $\alpha = 2 \times 10^{-4}$, and (d) $N = 8$ with $\alpha = 2 \times 10^{-5}$. The dashed circles indicate the optimal values of $|z|$ predicted by the analytic expression (15).

$N = 6$ sites. The WFMC simulations use per-site Fock cutoffs balancing accuracy and computational cost [62], and produce $g_s^{(2)}(0)$ from the full multiphoton state rather than its low-occupation approximation (13). The results shown here use drive amplitude $F_1 = 10^{-4}$, but almost identical outcomes are obtained for other choices of $F_1 \ll 1$ [62]. The WFMC and weak drive calculations give very similar results, particularly with regard to the parameter values where photon antibunching occurs. The results for $N = 2$ and $N = 4$ show similar good agreement, as shown in the Supplemental Material [62].

Figure 3(b) shows the unequal time second-order correlation $g_s^{(2)}(\tau)$ [62], calculated with WFMC for lattices of size $N = 2, 4, 6$ (with each lattice tuned to its optimal point). For $N = 2$ (a single dimer), the correlation has previously been shown to oscillate with τ [29]. The behavior for larger values of N is similar, with the oscillation frequency not significantly influenced by N. Till now, our discussion bases on a normalization $J = 1$. If we forgo the normalization and make J tunable, we can show that for the same nonlinearity strength, a longer dimer chain allows a smaller optimal J to achieve UPB. This indicates that a longer dimer chain allows for longer antibunching timescale, which is favorable in experiments [62].

In systems with significant environmental interactions, UPB may be constrained by pure dephasing processes such as coupling to background phonon modes [29,39,64], distinct from the dissipation-induced quantum jumps considered thus far. To investigate this, we performed a set of WFMC simulations with the term

$$i\frac{\kappa}{2}\sum_j (2a_j^\dagger a_j \rho a_j^\dagger a_j - a_j^\dagger a_j a_j^\dagger a_j \rho - \rho a_j^\dagger a_j a_j^\dagger a_j) \qquad (19)$$

added to the Lindblad master equation [29]. Figure 3(c) shows the z dependence of $g_s^{(2)}(0)$ for $N = 4$ using dephasing rates $\kappa = 10^{-3}\alpha$, 0.1α, and α. We find that excessively strong pure dephasing "smears out" the zeros of $g_s^{(2)}(0)$. Figure 3(d) plots the dependence of $g_s^{(2)}(0)$ on the dephasing rate for lattices of size $N = 2$, 4, and 6, indicating that photon antibunching requires κ to be small compared to α. This must be accounted for if UPB is to be achieved in large-N lattices with extremely weak nonlinearities. A previous study of silicon photonic crystal cavities estimated a pure dephasing rate of $\kappa \approx 10^{-7}\gamma$ at room temperature [39]; if so, even the $N = 8$ lattice, which requires $\alpha \approx 6.6 \times 10^{-5}\gamma$, would be in the regime of negligible pure dephasing.

The finding of exponential UPB enhancement points to interesting opportunities for using photonic lattices to manipulate multi-photon quantum states. The enhancement appears to stem from the exponential scaling of the number of spatial excitation pathways with lattice size; tiny shifts of these pathways, induced by an exponentially weak

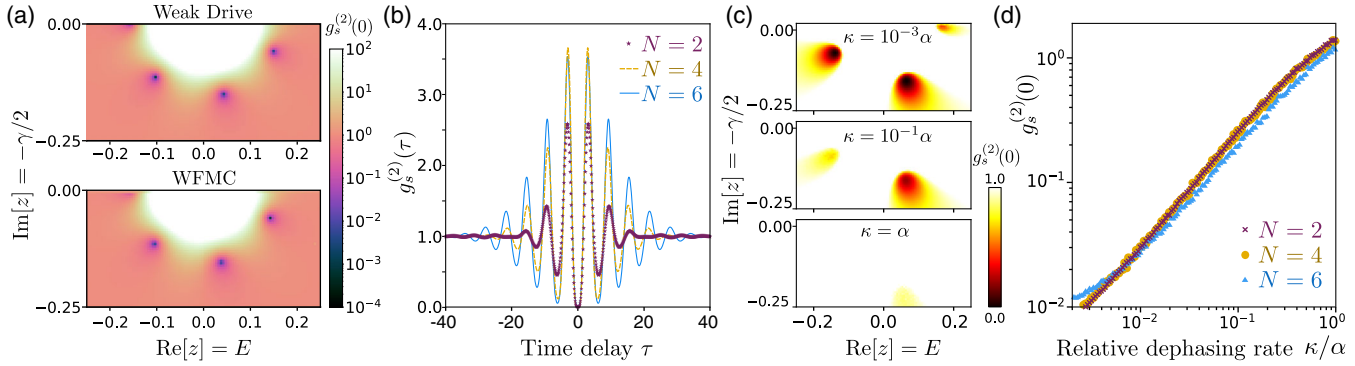

FIG. 3. Wave function Monte Carlo (WFMC) results. In all subplots, we take $t = 0.1$ and for lattices of size $N = 2$, 4, 6, we set $\alpha = 10^{-2}$, 2×10^{-3}, 2×10^{-4}, respectively. (a) Equal time second-order correlation $g_s^{(2)}(0)$ versus $z = E - i\gamma/2$ for a lattice of size $N = 6$, obtained using the weak drive equations without series expansions (upper panel), and using WFMC simulations with drive amplitude $F_1 = 10^{-4}$ (lower panel). The color scale for $g_s^{(2)}(0)$ is capped at 100 so that the minima can be more clearly seen. (b) WFMC results for the unequal time correlation $g_s^{(2)}(\tau)$. For each N, the value of z is chosen to minimize $g_s^{(2)}(0)$, and is located by doing simulations with different z on a discrete grid. The horizontal axis has units of $\hbar$ over the intracell coupling. In (a) and (b), the WFMC simulations do not include pure dephasing. (c) Plots of $g_s^{(2)}(0)$ versus z for a lattice with $N = 4$, obtained using WFMC simulations with dephasing rates $\kappa = 0.001\alpha$, 0.1α, α (top to bottom). To distinguish the local minima more clearly, all regions for which $g_s^{(2)}(0) \geq 1$ are colored white. (d) Dependence of $g_s^{(2)}(0)$ on κ/α for lattices of size $N = 2$, 4, 6, using the same values of z as in (b).

nonlinearity, can thereby achieve destructive interference of the two-photon amplitude in a signal cavity. More generally, the lattice's larger Hilbert space offers more room to find a global steady state in which the reduced density matrix at the signal cavity satisfies the relevant constraints. The chiral symmetry of the lattice also plays an important role in setting up the right interference conditions between single-photon eigenmodes in different bands [62]. In the future, related effects could be explored in more complicated systems such as two-dimensional lattices, as well as exploiting special lattice phenomena such as topologically protected single-photon states [65,66]. These ideas might also be used to implement single-photon sources using silicon photonics, or other photonic platforms with weak nonlinearities.

This work was supported by the Singapore MOE Academic Research Fund Tier 3 Grant MOE2016-T3-1-006, Tier 2 Grant MOE2019-T2-1-004, and Tier 1 Grant RG148/20, and by the National Research Foundation Competitive Research Programs NRF-CRP23-2019-0005 and NRF-CRP23-2019-0007.

*These authors contributed equally to this work.
†blzhang@ntu.edu.sg
‡timothyliew@ntu.edu.sg
§yidong@ntu.edu.sg

[1] L. Tian and H. J. Carmichael, Quantum trajectory simulations of two-state behavior in an optical cavity containing one atom, Phys. Rev. A **46**, R6801 (1992).
[2] W. Leoński and R. Tanaś, Possibility of producing the one-photon state in a kicked cavity with a nonlinear Kerr medium, Phys. Rev. A **49**, R20 (1994).
[3] A. Imamoğlu, H. Schmidt, G. Woods, and M. Deutsch, Strongly Interacting Photons in a Nonlinear Cavity, Phys. Rev. Lett. **79**, 1467 (1997).
[4] P. Lodahl, S. Mahmoodian, and S. Stobbe, Interfacing single photons and single quantum dots with photonic nanostructures, Rev. Mod. Phys. **87**, 347 (2015).
[5] E. Knill, R. Laflamme, and G. J. Milburn, A scheme for efficient quantum computation with linear optics, Nature (London) **409**, 46 (2001).
[6] K. M. Birnbaum, A. Boca, R. Miller, A. D. Boozer, T. E. Northup, and H. J. Kimble, Photon blockade in an optical cavity with one trapped atom, Nature (London) **436**, 87 (2005).
[7] M. J. Hartmann, F. G. S. L. Brandão, and M. B. Plenio, Strongly interacting polaritons in coupled arrays of cavities, Nat. Phys. **2**, 849 (2006).
[8] P. Kok, W. J. Munro, K. Nemoto, T. C. Ralph, J. P. Dowling, and G. J. Milburn, Linear optical quantum computing with photonic qubits, Rev. Mod. Phys. **79**, 135 (2007).
[9] R. O. Umucalılar and I. Carusotto, Fractional Quantum Hall States of Photons in an Array of Dissipative Coupled Cavities, Phys. Rev. Lett. **108**, 206809 (2012).
[10] C. Noh and D. G. Angelakis, Quantum simulations and many-body physics with light, Rep. Prog. Phys. **80**, 016401 (2016).
[11] B. Dayan, A. S. Parkins, T. Aoki, E. P. Ostby, K. J. Vahala, and H. J. Kimble, A photon turnstile dynamically regulated by one atom, Science **319**, 1062 (2008).
[12] C. Hamsen, K. N. Tolazzi, T. Wilk, and G. Rempe, Two-Photon Blockade in an Atom-Driven Cavity QED System, Phys. Rev. Lett. **118**, 133604 (2017).

[13] P. Michler, A. Kiraz, C. Becher, W. V. Schoenfeld, P. M. Petroff, L. Zhang, E. Hu, and A. Imamoğlu, A quantum dot single-photon turnstile device, Science **290**, 2282 (2000).
[14] A. Faraon, I. Fushman, D. Englund, N. Stoltz, P. Petroff, and J. Vučković, Coherent generation of nonclassical light on a chip via photon-induced tunnelling and blockade, Nat. Phys. **4**, 859 (2008).
[15] J. Claudon, J. Bleuse, N. S. Malik, M. Bazin, P. Jaffrennou, N. Gregersen, C. Sauvan, P. Lalanne, and J.-M. Gérard, A highly efficient single-photon source based on a quantum dot in a photonic nanowire, Nat. Photonics **4**, 174 (2010).
[16] Y.-M. He, Y. He, Y.-J. Wei, D. Wu, M. Atatüre, C. Schneider, S. Höfling, M. Kamp, C.-Y. Lu, and J.-W. Pan, On-demand semiconductor single-photon source with near-unity indistinguishability, Nat. Nanotechnol. **8**, 213 (2013).
[17] K. H. Madsen, S. Ates, J. Liu, A. Javadi, S. M. Albrecht, I. Yeo, S. Stobbe, and P. Lodahl, Efficient out-coupling of high-purity single photons from a coherent quantum dot in a photonic-crystal cavity, Phys. Rev. B **90**, 155303 (2014).
[18] M. Gschrey, A. Thoma, P. Schnauber, M. Seifried, R. Schmidt, B. Wohlfeil, L. Krüger, J. H. Schulze, T. Heindel, S. Burger, F. Schmidt, A. Strittmatter, S. Rodt, and S. Reitzenstein, Highly indistinguishable photons from deterministic quantum-dot microlenses utilizing three-dimensional in situ electron-beam lithography, Nat. Commun. **6**, 7662 (2015).
[19] N. Somaschi, V. Giesz, L. D. Santis, J. C. Loredo, M. P. Almeida, G. Hornecker, S. L. Portalupi, T. Grange, C. Antón, J. Demory, C. Gómez, I. Sagnes, N. D. Lanzillotti-Kimura, A. Lemaítre, A. Auffeves, A. G. White, L. Lanco, and P. Senellart, Near-optimal single-photon sources in the solid state, Nat. Photonics **10**, 340 (2016).
[20] C. Dory, K. A. Fischer, K. Müller, K. G. Lagoudakis, T. Sarmiento, A. Rundquist, J. L. Zhang, Y. Kelaita, N. V. Sapra, and J. Vučković, Tuning the photon statistics of a strongly coupled nanophotonic system, Phys. Rev. A **95**, 023804 (2017).
[21] N. Jia, N. Schine, A. Georgakopoulos, A. Ryou, L. W. Clark, A. Sommer, and J. Simon, A strongly interacting polaritonic quantum dot, Nat. Phys. **14**, 550 (2018).
[22] C. Lang, D. Bozyigit, C. Eichler, L. Steffen, J. M. Fink, A. A. Abdumalikov, M. Baur, S. Filipp, M. P. da Silva, A. Blais, and A. Wallraff, Observation of Resonant Photon Blockade at Microwave Frequencies Using Correlation Function Measurements, Phys. Rev. Lett. **106**, 243601 (2011).
[23] X. Wang, A. Miranowicz, H.-R. Li, and F. Nori, Multiple-output microwave single-photon source using superconducting circuits with longitudinal and transverse couplings, Phys. Rev. A **94**, 053858 (2016).
[24] P. Rabl, Photon Blockade Effect in Optomechanical Systems, Phys. Rev. Lett. **107**, 063601 (2011).
[25] X.-W. Xu, A.-X. Chen, and Y.-x. Liu, Phonon blockade in a nanomechanical resonator resonantly coupled to a qubit, Phys. Rev. A **94**, 063853 (2016).
[26] M.-A. Lemonde, N. Didier, and A. A. Clerk, Enhanced nonlinear interactions in quantum optomechanics via mechanical amplification, Nat. Commun. **7**, 11338 (2016).
[27] A. Majumdar, M. Bajcsy, A. Rundquist, and J. Vučković, Loss-Enabled Sub-Poissonian Light Generation in a Bimodal Nanocavity, Phys. Rev. Lett. **108**, 183601 (2012).
[28] A. Majumdar and D. Gerace, Single-photon blockade in doubly resonant nanocavities with second-order nonlinearity, Phys. Rev. B **87**, 235319 (2013).
[29] T. C. H. Liew and V. Savona, Single Photons from Coupled Quantum Modes, Phys. Rev. Lett. **104**, 183601 (2010).
[30] S. Ferretti, L. C. Andreani, H. E. Türeci, and D. Gerace, Photon correlations in a two-site nonlinear cavity system under coherent drive and dissipation, Phys. Rev. A **82**, 013841 (2010).
[31] M. Bamba, A. Imamoğlu, I. Carusotto, and C. Ciuti, Origin of strong photon antibunching in weakly nonlinear photonic molecules, Phys. Rev. A **83**, 021802(R) (2011).
[32] M. Bamba and C. Ciuti, Counter-polarized single-photon generation from the auxiliary cavity of a weakly nonlinear photonic molecule, Appl. Phys. Lett. **99**, 171111 (2011).
[33] H. Flayac and V. Savona, Input-output theory of the unconventional photon blockade, Phys. Rev. A **88**, 033836 (2013).
[34] X.-W. Xu and Y. Li, Strong photon antibunching of symmetric and antisymmetric modes in weakly nonlinear photonic molecules, Phys. Rev. A **90**, 033809 (2014).
[35] M.-A. Lemonde, N. Didier, and A. A. Clerk, Antibunching and unconventional photon blockade with gaussian squeezed states, Phys. Rev. A **90**, 063824 (2014).
[36] H. J. Snijders, J. A. Frey, J. Norman, H. Flayac, V. Savona, A. C. Gossard, J. E. Bowers, M. P. van Exter, D. Bouwmeester, and W. Löffler, Observation of the Unconventional Photon Blockade, Phys. Rev. Lett. **121**, 043601 (2018).
[37] C. Vaneph, A. Morvan, G. Aiello, M. Féchant, M. Aprili, J. Gabelli, and J. Estève, Observation of the Unconventional Photon Blockade in the Microwave Domain, Phys. Rev. Lett. **121**, 043602 (2018).
[38] D. Gerace and V. Savona, Unconventional photon blockade in doubly resonant microcavities with second-order nonlinearity, Phys. Rev. A **89**, 031803(R) (2014).
[39] H. Flayac, D. Gerace, and V. Savona, An all-silicon single-photon source by unconventional photon blockade, Sci. Rep. **5**, 11223 (2015).
[40] H. Flayac and V. Savona, Unconventional photon blockade, Phys. Rev. A **96**, 053810 (2017).
[41] G. Wang, H. Z. Shen, C. Sun, C. Wu, J.-L. Chen, and K. Xue, Unconventional photon blockade in weakly nonlinear photonic molecules with bilateral drive, J. Mod. Opt. **64**, 583 (2017).
[42] S. Ghosh and T. C. H. Liew, Single photons from a gain medium below threshold, Phys. Rev. B **97**, 241301(R) (2018).
[43] B. Sarma and A. K. Sarma, Unconventional photon blockade in three-mode optomechanics, Phys. Rev. A **98**, 013826 (2018).
[44] S. Ghosh and T. C. H. Liew, Dynamical Blockade in a Single-Mode Bosonic System, Phys. Rev. Lett. **123**, 013602 (2019).
[45] H. Carmichael, R. Brecha, and P. Rice, Quantum interference and collapse of the wavefunction in cavity QED, Opt. Commun. **82**, 73 (1991).

[46] M. Radulaski, K. A. Fischer, K. G. Lagoudakis, J. L. Zhang, and J. Vučković, Photon blockade in two-emitter-cavity systems, Phys. Rev. A **96**, 011801(R) (2017).
[47] K. Kamide, Y. Ota, S. Iwamoto, and Y. Arakawa, Method for generating a photonic noon state with quantum dots in coupled nanocavities, Phys. Rev. A **96**, 013853 (2017).
[48] E. Zubizarreta Casalengua, J. C. López Carreño, F. P. Laussy, and E. del Valle, Conventional and unconventional photon statistics, Laser Photonics Rev. **14**, 1900279 (2020).
[49] T. C. H. Liew and V. Savona, Quantum entanglement in nanocavity arrays, Phys. Rev. A **85**, 050301(R) (2012).
[50] T. C. H. Liew and V. Savona, Multimode entanglement in coupled cavity arrays, New J. Phys. **15**, 025015 (2013).
[51] J. D. Joannopoulos, S. G. Johnson, J. N. Winn, and R. D. Meade, *Photonic Crystals* (Princeton University Press, Princeton, 2008).
[52] J. B. Pendry, Negative Refraction Makes a Perfect Lens, Phys. Rev. Lett. **85**, 3966 (2000).
[53] E. Shamonina and L. Solymar, Metamaterials: How the subject started, Metamaterials **1**, 12 (2007).
[54] C. W. Hsu, B. Zhen, A. D. Stone, J. D. Joannopoulos, and M. Soljačić, Bound states in the continuum, Nat. Rev. Mater. **1**, 16048 (2016).
[55] W. P. Su, J. R. Schrieffer, and A. J. Heeger, Solitons in Polyacetylene, Phys. Rev. Lett. **42**, 1698 (1979).
[56] S. Ferretti, V. Savona, and D. Gerace, Optimal antibunching in passive photonic devices based on coupled nonlinear resonators, New J. Phys. **15**, 025012 (2013).
[57] H. Breuer and F. Petruccione, *The Theory of Open Quantum Systems* (Oxford University Press, Oxford, 2007); H. Carmichael, *Statistical Methods in Quantum Optics 2: Non-Classical Fields* (Springer, Berlin Heidelberg, 2007).
[58] A. Barchielli and V. P. Belavkin, Measurements continuous in time and a posteriori states in quantum mechanics, J. Phys. A **24**, 1495 (1991).
[59] R. Dum, A. S. Parkins, P. Zoller, and C. W. Gardiner, Monte Carlo simulation of master equations in quantum optics for vacuum, thermal, and squeezed reservoirs, Phys. Rev. A **46**, 4382 (1992).
[60] K. Mølmer, Y. Castin, and J. Dalibard, Monte Carlo wave-function method in quantum optics, J. Opt. Soc. Am. B **10**, 524 (1993).
[61] H. Carmichael, *An Open Systems Approach to Quantum Optics* (Springer, New York, 1993).
[62] See Supplemental Material at http://link.aps.org/supplemental/10.1103/PhysRevLett.127.240402 for details of the analytic derivations based on the weak drive approximation and the wave function Monte Carlo simulations.
[63] S. Krämer, D. Plankensteiner, L. Ostermann, and H. Ritsch, QuantumOptics.jl: A Julia framework for simulating open quantum systems, Comput. Phys. Commun. **227**, 109 (2018).
[64] C. Piermarocchi, V. Savona, A. Quattropani, P. Schwendimann, and F. Tassone, Photoluminescence and carrier dynamics in gaas quantum wells, Phys. Status. Solidi A **164**, 221 (1997).
[65] T. Ozawa, H. M. Price, A. Amo, N. Goldman, M. Hafezi, L. Lu, M. C. Rechtsman, D. Schuster, J. Simon, O. Zilberberg, and I. Carusotto, Topological photonics, Rev. Mod. Phys. **91**, 015006 (2019).
[66] D. Smirnova, D. Leykam, Y. Chong, and Y. Kivshar, Nonlinear topological photonics, Appl. Phys. Rev. **7**, 021306 (2020).